

Revista Mexicana de Astronomía y Astrofísica
Universidad Nacional Autónoma de México
rmaa@astroscu.unam.mx
ISSN (Versión impresa): 0185-1101
MÉXICO

2001

G. Koenigsberger / F. Cervantes / E. Moreno / L. Georgiev
TIDAL FORCES AND THE MASS-LOSS HISTORY OF BINARY STARS
Revista Mexicana de Astronomía y Astrofísica, número 010
Universidad Nacional Autónoma de México
Distrito Federal, México
pp. 199-204

Red de Revistas Científicas de América Latina y el Caribe, España y Portugal

Universidad Autónoma del Estado de México

<http://redalyc.uaemex.mx>



TIDAL FORCES AND THE MASS-LOSS HISTORY OF BINARY STARS

G. Koenigsberger, F. Cervantes, E. Moreno, and L. Georgiev

Instituto de Astronomía, Universidad Nacional Autónoma de México

RESUMEN

Analizamos el papel que juegan las fuerzas de marea en la evolución de la pérdida de masa en sistemas binarios. Las fuerzas de marea producen oscilaciones en la superficie de las estrellas que no se encuentran en corrotación o bien cuyas órbitas son excéntricas. Usando un modelo numérico bidimensional sencillo, mostramos la dependencia de las amplitudes de oscilación con el radio estelar y con la velocidad angular de rotación. Dado que las amplitudes de oscilación se incrementan rápidamente con un incremento en el radio estelar, fases importantes de pérdida de masa deben presentarse poco después de que la estrella deja la secuencia principal. Sugerimos que las trazas evolutivas de estrellas que forman parte de sistemas binarios fuera de equilibrio podrían diferir en forma significativa de las trazas evolutivas para estrellas aisladas.

ABSTRACT

The role played by tidal forces in shaping the mass-loss history of binary stars is discussed. Tidal forces drive oscillations on the surface of stars whose rotation and orbital periods are not synchronized and/or whose orbits are eccentric. Using a simple, two-dimensional numerical model, we show how the oscillation amplitudes depend on the star's radius and its rotational angular velocity in a given system. Except for synchronous systems, our models for circular orbits result in oscillating stellar surfaces, with periods depending on the ratio of the spin to the orbital angular velocities. In the case of eccentric systems, as the star spins-down (or spins-up) due to tidal torques, large amplitude oscillations are predicted when a resonance between the spin and orbital angular velocities is encountered, suggesting the occurrence of numerous episodes of enhanced mass-loss in its circularization timescale. Because the amplitudes of the oscillations increase rapidly with an increasing stellar radius, tidal oscillations will most likely drive a phase of rapid and probably non-spherically symmetric mass-loss as the star leaves the main sequence and expands. Furthermore, enhanced mass-loss rates might be expected even from MS stars in non-equilibrium binary systems, when compared with analogous single stars. Thus, we suggest that the mass-loss history and the post-MS evolutionary tracks followed by stars in non-equilibrium binary systems may differ significantly from those of single stars. Systems such as η Carinae and the Wolf-Rayet/Luminous Blue Variable HD 5980 may be displaying the consequences of tidally driven pulsations.

Key Words: **BINARIES: GENERAL — STARS: MASS LOSS — STARS: VARIABLE: GENERAL**

1. INTRODUCTION

The mass-loss history of massive stars is closely connected to their evolution. Four general stages can be defined: 1) persistent, radiation-pressure driven winds during the Main Sequence (MS); 2) sudden eruptive events after the star leaves the MS, associated with a slow wind, and believed to correspond to the Luminous Blue Variable evolutionary phase in massive stars; 3) radiation-driven fast wind phases during subsequent core He,C-burning stages, generally associated with Wolf-Rayet (WR) stars; and 4) the supernova (SN) explosion.

The actual mass–loss rates depend upon the properties (i.e., mass, radius, effective temperature, metallicity, stellar rotation) of the underlying star (see review by Kudritzki & Puls 2000), properties which are changing as the star evolves. In binaries (which constitute $\sim 50\%$ of all stars), interaction effects between the two components also play a role. Tidal forces are responsible for the evolution of the orbital parameters, and when the orbit is eccentric and/or when the orbital and rotational periods are not synchronized, tidal forces drive the system towards an equilibrium state through the transfer between orbital and rotational angular momentum and energy (see, for example, Zahn 1989, and references therein).

The theoretical computations of post–MS massive star evolution, include a rapid phase of mass loss through the classical Roche Lobe Overflow (RLO) scenario (see, for example, de Greve 1996). However, the RLO models are valid only for equilibrium conditions. But circularization timescales are, in general, too long compared with MS lifetimes of massive stars for an equilibrium state to have been achieved before the star leaves the MS. Thus, we propose that, as the star’s radius increases, and the amplitude of the tidal oscillations grow, it is very likely that a significant mass–shedding series of events will occur before the star’s radius reaches the dimensions of the classical Roche Lobe, preventing it from ever reaching it.

In this paper we discuss some of the (instantaneous) effects that tidal forces produce on the surface layers of stars in binary systems, and the dependence of these effects on the stellar radius and rotation velocity. A model of eruptions driven by tidal oscillations might be applicable to binary systems such as HD 5980 in the SMC (Koenigsberger et al. 1999), η Carinae, and the 7.9 year periodic eruptor WR 140, among others.

2. DESCRIPTION OF THE MODEL

We have developed a simple two–dimensional tidal interaction model in which stellar rotation is included (Moreno & Koenigsberger 1999). The two stars in the binary system have masses m_1 and m_2 , and radii R_1 and R_2 . The orbit has a semi–major axis a and eccentricity e . The stellar rotation is characterized by the parameter $\beta = \omega/\Omega$, where ω and Ω are the stellar rotation angular velocity and the orbital angular velocity, respectively. The equators of both stars are assumed to lie in the orbital plane. Each of the stars is analyzed separately by solving the equation of motion for (in this paper) 100 surface elements located along the equator in a thin shell. This thin shell lies deep enough within the atmosphere so that the oscillations can be treated as adiabatic, but high enough so that the amount of mass lying above it is negligible. The main body of the star, interior to the shell, is assumed to behave as a rigid body and the tidal deformation is assumed to occur mainly in the external shell. Clearly, this approximation of the responding region of the star to only one thin shell is a simplified picture of the true phenomenon. In reality, all layers of the star are subjected to the tidal forces, and the interaction between the response of each layer with its underlying and overlying layers will determine the overall behavior at the oscillations. However, the model provides a general picture of the role that the different physical forces play in distorting the stellar surface, and the dependence of this deformation on the values of the stellar and orbital parameters, and on the viscosity of the gas. For more general models, the reader is referred to, for example, Kumar, Ao & Quataert (1995), Willems et al. (1997), and references therein.

In the non–inertial reference system centered on m_1 and rotating with the orbital angular velocity Ω , the equation of motion to solve for each element on the surface of the equatorial shell of m_1 is:

$$\begin{aligned} \mathbf{a}' &= \mathbf{a}_{\text{INT}} - \frac{Gm_1\mathbf{r}'}{|\mathbf{r}'|^3} - Gm_2 \left[\frac{\mathbf{r} - \mathbf{r}_2}{|\mathbf{r} - \mathbf{r}_2|^3} + \frac{\mathbf{r}_2 - \mathbf{r}_1}{|\mathbf{r}_2 - \mathbf{r}_1|^3} \right] - \\ &- \Omega \times (\Omega \times \mathbf{r}') - 2\Omega \times \mathbf{v}' - \frac{d\Omega}{dt} \times \mathbf{r}'. \end{aligned} \quad (1)$$

where \mathbf{a}_{INT} is the total inertial acceleration on the element, other than the gravitational due to m_1 and m_2 ; \mathbf{r} , \mathbf{r}_1 , \mathbf{r}_2 are the positions, respectively, of the surface element, of m_1 , and of m_2 , with respect to an inertial system; and \mathbf{r}' , \mathbf{v}' are the position and velocity of the element in the non–inertial frame.

In the non–gravitational inertial acceleration \mathbf{a}_{INT} we include the following forces: (i) the internal outward gas pressure force on the surface element, (ii) the lateral azimuthal force on the element due to possible different gas pressures exerted by adjacent elements, and (iii) the radial and azimuthal viscous forces exerted by adjacent azimuthal elements and by material below the given element, respectively. A more detailed description of the model and method of solution can be found in Moreno & Koenigsberger (1999).

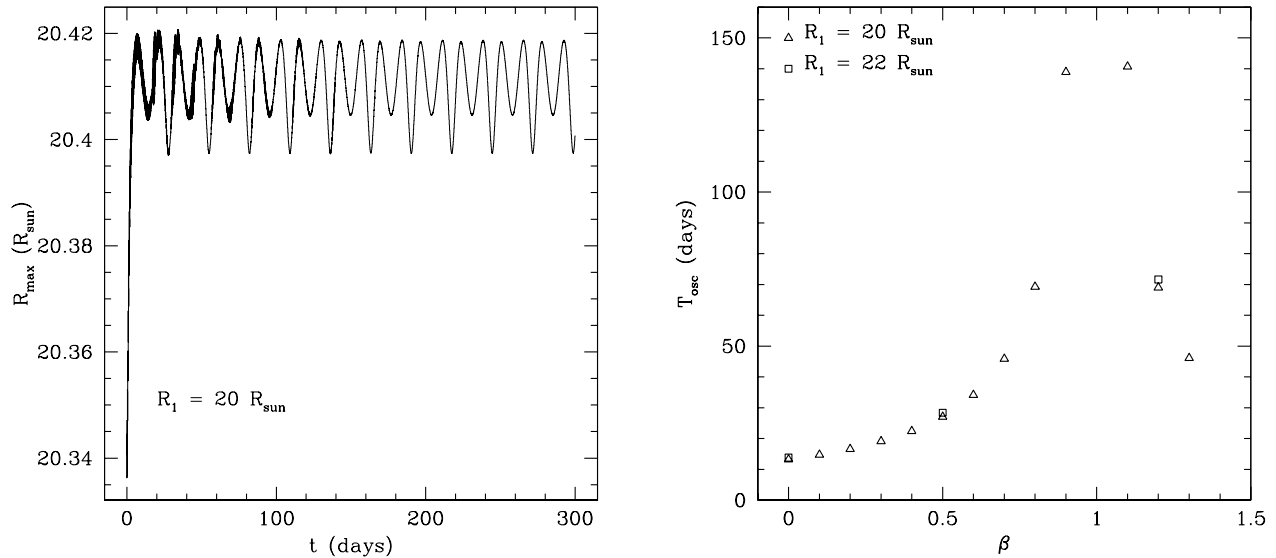


Fig. 1. Oscillations of the maximum stellar radius. (a) Behavior of R_{max} as a function of time for the $20 R_{\odot}$ model and $\beta=0.4$ (sub-synchronous rotation). The oscillation period is 22.43 days, although the orbital period is only 12.95 days. (b) Oscillation period of the maximum radius as a function of β . At $\beta=1$, no oscillations are present. Triangles and squares indicate computations with different stellar radii, as indicated.

The degree of surface deformation is quantified using the parameter $R_{max} = \max[R_i]$, the maximum radius achieved by the star in a given direction at any given time. The radii R_i correspond to the 100 individual surface elements, with R_1 belonging to the surface element which faces the companion at the time the calculation is started. The “tidal bulge” coincides with the set of surface elements that include R_{max} , and in systems that are close to an equilibrium configuration, the bulge is oriented in the general direction of the companion. Far from equilibrium, for large values of the rotational velocity, however, at any given time the R_{max} element may be oriented in any direction because of the modes in which the oscillations are driven. We define the angle Θ_{bulge} to denote the position of the element at which R_{max} is attained. This angle is measured with respect to the line joining the centers of the two stars. The maximum radial velocity amplitude is quantified using the parameter $(v_r)_{max} = \max[v_i]$. At any given time, the surface element with the largest radius (i.e., R_{max}) and the surface element with the largest outward velocity (i.e., $(v_r)_{max}$) are different surface elements.

3. TIDAL OSCILLATIONS AND STELLAR ROTATION IN CIRCULAR ORBITS

In this section we explore the behavior of the tidally induced oscillations as a function of $\beta = \omega/\Omega$, the ratio of spin to orbital angular velocity, for values of $\beta=0.0-3.0$. The model binary system that is used consists of two $40 M_{\odot}$ stars in a circular orbit, with separation $a=100 R_{\odot}$, so that its orbital period is 12.95 days. The radius of the star to be analyzed is $R_1=20 R_{\odot}$, and we set a depth of $0.01 \times R_1$ for the layer that is allowed to be deformed. The kinematic viscosity (Landau and Lifshitz 1984) assumed for these calculations is $\nu=0.2 R_{\odot}^2 \text{ day}^{-1}$, which corresponds to values of the dynamical viscosity, $\eta \sim 1 \times 10^{12} \text{ gm cm}^{-1} \text{ s}^{-1}$ for surface densities typical of giant stars, or to values $\sim 1 \times 10^{14} \text{ gm cm}^{-1} \text{ s}^{-1}$ for surface densities typical of main sequence stars.

Figure 1a illustrates the behavior of R_{max} as a function of time. The calculation is started at $t=0$, and after a brief transitory phase, a smooth, double-maximum, periodic pulsation is present. For the case illustrated in Figure 1a ($\beta=0.4$), $P_{pulse}=22.43$ days, the total amplitude of R_{max} is $\sim 0.02 R_{\odot}$, and the total amplitude of $(v_r)_{max}$ is $\sim 0.4 \text{ km/s}$. The location of the tidal bulge, where the large amplitude in R_{max} is present, is approximately -15 deg (i.e., it is “lagging” behind) while the location of the largest radial velocity amplitudes is

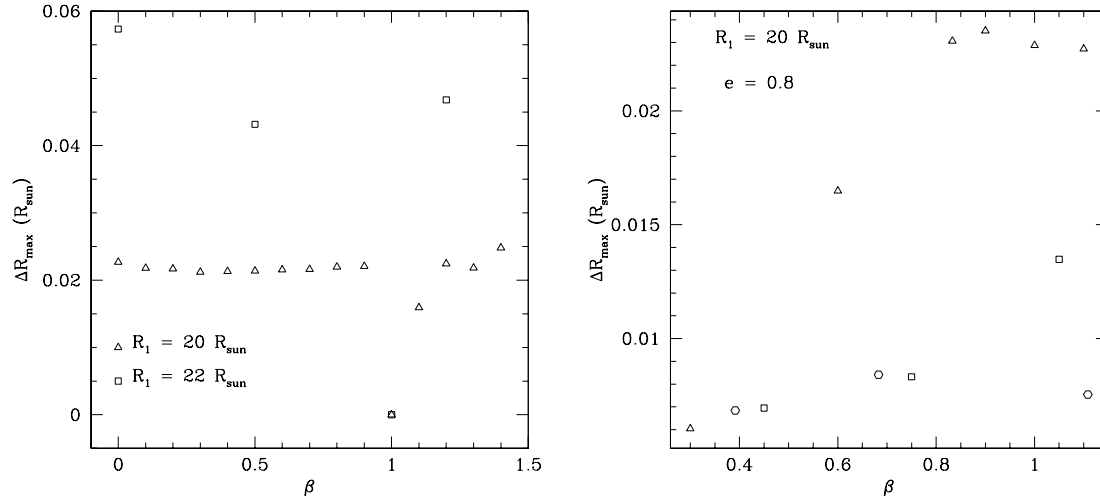


Fig. 2. Radial displacement amplitudes of the maximum radius as a function of β . (a) **circular orbits**: Triangles correspond to the $20 R_{\odot}$ model and squares to the $22 R_{\odot}$ model. There is a significant increase in amplitudes for the larger star. No oscillations are present when spin and orbital periods are synchronized. (b) **eccentric orbits**: the $20 R_{\odot}$ model in an eccentric ($e=0.8$) orbit with a major semi-axis $a=500 R_{\odot}$. Large amplitude oscillations appear at the resonances between the spin and the orbital angular velocity (triangles), with smaller amplitudes at non-resonant configurations (circles and squares).

at approximately $+20$ deg (see Figure 3a). Hence, if this were an eclipsing binary system, the best time to detect large scale photospheric motions would be before the eclipse of the oscillating star. It is important to note, however, that the location at which maximum amplitudes occur varies as a function of β . For sub-synchronous systems, $\Theta_{bulge} < 0$, but for super-synchronous systems, $\Theta_{bulge} > 0$.

The pulsation period driven by the tidal forces also depends on β , as illustrated in Figure 1b. For $\beta=0$, the period of oscillation is equal to the orbital period. For larger values of β , the period grows until β approaches unity, where no oscillations are present. For larger β , the period decreases again, but for $\beta > 1.6$, high frequency oscillations appear and grow in amplitude until they completely dominate the temporal variability behavior.

The dependence on β of the radial displacements of the surface elements is illustrated in Figure 2a, where the amplitude of R_{max} is plotted. These amplitudes remain fairly similar for $\beta < 1$. At $\beta=1$ they become zero. For $\beta > 1.4$ the amplitudes grow rapidly, as the high frequency oscillations begin to dominate. For the binary parameters considered in these calculations, $\beta \sim 3$ seems to be an upper limit for coherent oscillations, with effects that could be associated with turbulence setting in for the high stellar rotation rates.

Figure 3a illustrates the radial velocity amplitude for each of the 100 surface elements included in the computations. The companion star is located to the right in this figure, at coordinates (100, 0). Note that in this two-dimensional figure, there are apparently four nodes, where the velocity is zero. In three-dimensional space, this configuration is a cross-section at the equatorial plane. All our $\beta < 2$ models produce this mode of oscillations, suggestive of a superposition of non-radial models with the possible dominance of $l=2$, $m=2$ configurations.

The behavior of $(v_r)_{max}$ as a function of β is illustrated in Figure 3b. Velocities larger than 1.2 km/s are achieved for cases with β either very small or large. The amplitudes of both R_{max} and $(v_r)_{max}$ increase with increasing stellar radius, as is illustrated in Figures 2a and 3b, where the results of a few model runs with $R_1=22 R_{\odot}$ are plotted with a different symbol (squares) than the $R_1=20 R_{\odot}$ model. The pulsation periods, however, do not vary significantly (see Figure 1b).

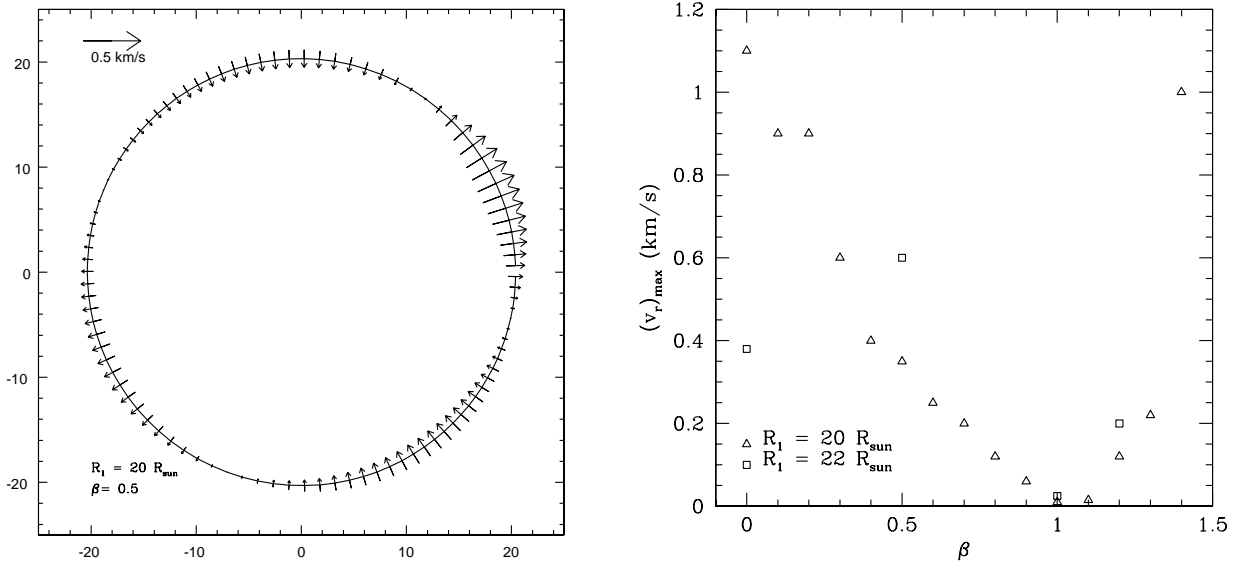


Fig. 3. Radial velocity amplitudes of the surface elements: (a) Radial velocity amplitudes of the individual surface elements for the case of $\beta=0.5$. (b) Maximum radial velocity as a function of β . Squares and triangles as in Figure 2a.

4. ECCENTRIC ORBITS

As spin and orbital angular momentum and energy are transferred in an eccentric binary system through the torques produced by the tides, the eccentricity is expected to decrease, and the system is expected to approach an equilibrium state. However, this appears not to be a smooth process, unless the system first becomes circularized, and then it is forced into corotation. This is because the eccentric systems have a series of resonances that occur when the surface element facing the companion at periastron returns to this same position after each orbital cycle, and a second series of resonances for this configuration, half a cycle after. Figure 2b illustrates the different values of the R_{max} amplitudes at the resonances (triangles indicating the resonance) and for non-resonant spin-orbit configurations (circles and squares). Note the increase in the amplitudes for the resonant cases, and particularly the primary resonances. This means that an eccentric system which is changing its spin angular velocity, will encounter these resonances and possibly undergo a phase of enhanced mass loss. This will probably modify its subsequent spin-down or spin-up rate.

5. CONCLUSIONS

We have explored the impact that tidal forces have on the surface layer of a star that forms part of a non-equilibrium binary configuration; i.e., it is either not co-rotating in a circular orbit, or it is in an eccentric orbit. Under these conditions, surface oscillations are excited. We apply a simple two-dimensional model to quantify, if ever so crudely, the dependence of the oscillation amplitudes on several of the binary system's parameters. We find that the oscillation amplitudes depend strongly on the stellar radius and on the ratio of rotational to orbital angular velocity, $\beta=\omega/\Omega$. Thus, large amplitude oscillations may be present even on a slowly rotating star, if β departs significantly from unity, although the fast rotators are, indeed, the most unstable systems.

For circular orbits and $0 < \beta < 1.5$ (excluding $\beta=1$), the tidal forces produce a double peaked, periodic pulsation of the tidal bulge region with periods $P \sim P_{orb}$ and larger. Superimposed, higher frequency oscillations become evident for values $\beta > 1.0$, growing in amplitude until they dominate completely for $\beta > 1.5$, leading finally to the disruption of the model stellar surface at $\beta \sim 3$. At this point, we can no longer proceed with the computations. For eccentric orbits, the resonances which occur between the spin and orbital rotation rates

lead to a non-monotonic behavior of the oscillation amplitudes as a function of β . Thus, during the spin-down or spin-up history of an eccentric-orbit binary system, numerous unstable configurations will be encountered, and thus, a smooth transition towards an equilibrium configuration is not expected.

Surface oscillations can play a non-negligible role in modulating or otherwise interacting with wind instabilities (Castor 1986; Owocki, Castor & Rybicki 1988), as well as providing an additional source of energy and momentum that can be transferred to the wind, thereby enhancing mass-loss rates (Willson 1986). We suggest that stars in non-equilibrium close binary systems are most likely to start shedding their outer layers, through oscillations induced by the tidal forces, even while on the main sequence, adding to the mass-loss rates being driven by radiation pressure. As the star leaves the MS, the tidal effects will be enhanced, with possible eruptive mass-shedding events prevailing, and thus preventing the star from ever approaching the Roch Lobe configuration.

Rotation and its effects on the evolutionary path is a complex problem (see Heger et al. 2000) in itself. The inclusion of the binary interaction effects into the evolutionary computations adds to this already difficult problem. However, because the mass-loss history of a star determines the post-MS path it will follow, it is crucial to quantify the impact that tidal effects produce on the mass-loss history of the star. A full understanding of the post-MS evolutionary phases is needed for numerous problems such as determining the characteristics of starburst regions, supernovae explosions, the formation of black holes, and the role of collapsing stars in producing the extragalactic gamma ray bursts, and binaries may be playing a non-negligible role in most of these.

As a final comment regarding the roles of tidal oscillations, it is interesting to note that binary WR stars have stronger X-ray emission than comparable single stars (Pollock 1994). It is tempting to speculate that part of the excess X-ray emission observed in WR binary systems, may be produced in the shocks that are embedded in the stellar winds of the O-star companions to these WR stars.

We wish to express our gratitude to N. Langer for discussions held at early stages of this investigation, and for his always useful comments and suggestions. We acknowledge support from CONACYT grant 27744-E.

REFERENCES

- Castor, J. I. 1986, PASP 98, 52.
 de Greve, J. P. 1996, in Wolf-Rayet Stars in the Framework of Stellar Evolution, Proceedings of the 33rd Liège International Astrophysical Colloquium, eds. J. M. Vreux, A. Detal, D. Fraipont-Caro, E. Gosset & G. Rauw, p. 55.
 Heger, A. et al. 2000, ApJ 528,368.
 Koenigsberger, G., Moreno, E., Cantó, J. & Raga, A. 1999, in IAU Symposium 163, Wolf-Rayet Stars: Binaries, Colliding Winds, Evolution, eds. K. A. van der Hucht & P. M. Williams, Kluwer Academic Publishers, (Dordrecht) p.55.
 Kumar, P., Ao, C. O. & Quataert, E. J. 1995, ApJ 449, 294.
 Kudritzki, R. P. & Puls, J. 2000, ARA& A, 38, 613
 Landau, L. D. & Lifshitz, E. M. 1984, Fluid Mechanics, (Oxford:Pergamon Press).
 Moreno, E. & Koenigsberger, G. 1999, RMA&A, 35, 157.
 Owocki, S. P., Castor, J. I. & Rybicki, G. B. 1988, ApJ 335, 914.
 Pollock, A. M. T. 1994, in IAU Symposium 163, Wolf-Rayet stars: Binaries, Colliding winds, Evolution, eds. K. A. van der Hucht & P. M. Williams, Kluwer Academic Publishers, (Dordrecht) p.429
 Willems, B., van Hoolst, T., Smeyers, P. & Waelkens, C. 1997, A&A 326, L37.
 Willson, L. A. 1986, PASP 98, 37.
 Zahn, J.-P. 1989, A&A 220, 112

Fausto Cervantes, Leonid Georgiev, Gloria Koenigsberger, Edmundo Moreno: Instituto de Astronomía, Universidad Nacional Autónoma de México, Apdo. Postal 70-264, México D.F. 04510 (gloria,edmundo,fausto,georgiev@astroscu.unam.mx).